# Coupling among three chemical oscillators: Synchronization, phase death, and frustration

Minoru Yoshimoto
*Department of Chemistry, Faculty of Science, Nagoya University, Nagoya 464-01, Japan*

Kenichi Yoshikawa*
*Graduate School of Human Informatics, Nagoya University, Nagoya 464-01, Japan*

Yoshihito Mori
*Institute for Molecular Science, Okazaki 444, Japan*

(Received 14 August 1992; revised manuscript received 2 November 1992)

Various modes in three coupled chemical oscillators in a triangular arrangement were observed. As a well-defined nonlinear oscillator, the Belousov-Zhabotinsky reaction was studied in a continuous-flow stirred tank reactor (CSTR). Coupling among CSTR's was performed by mass exchange. The coupling strength was quantitatively controlled by changing the flow rate of reacting solutions among the three CSTR's using peristaltic pumps between each pair of the reactors. As a key parameter to control the model of coupling, we changed the symmetry of the interaction between the oscillators. In the case of the symmetric coupling, a quasiperiodic state or a biperiodic mode, an all-death mode and two kinds of synchronized modes appeared, depending on the coupling strength. On the other hand, under the asymmetric coupling, a quasiperiodic state or a biperiodic mode, an all death mode and four kinds of synchronized modes appeared. Those modes have been discussed in relation to the idea of "frustration" in the Ising spin system, where the three-phase mode appears as a transition from the Ising spin system to the $XY$ spin system.

PACS number(s): 05.40.+j, 05.70.Ln, 87.10.+e

## I. INTRODUCTION

Synchronization among nonlinear oscillators often plays an essential role in living organisms. Various kinds of rhythms in living systems, such as heart cells, neural cells, and metabolism for cellular calcium concentration, exhibit synchronization [1]. Synchronization has been the object of much study, including not only experimental but also physical and mathematical efforts. Besides the biological system, there have also been numerous studies in chemistry, electrical engineering, and physics. Especially among the chemical oscillators, coupling in the Belousov-Zhabotinsky (BZ) reaction and its modified versions has been extensively studied [2–16]. Marek and Stuchl [4] studied the coupling between two continuous-flow stirred tank reactors (CSTR's) by passive mass transfer through a perforated wall. When oscillators with different periods were coupled to each other, various synchronized modes arose: the in-phase mode, 1:2 synchronization, etc. Crowley and Epstein [11] studied the coupling between CSTR's by using a device to adjust the pore size for passive flow, in order to investigate the synchronization depending on the coupling flow rate. They found three kinds of synchronized modes: the antiphase mode, the in-phase mode, and the phase-death mode. In these previous studies, coupling between the reactors has been performed only in a passive manner through a pore between them except for the study of Laplante and Erneux on the coupled bistable reactors [15]. Recently, we have studied the coupling between two CSTR's, using a peristaltic pump to control the flow rate in a quantitative manner. We found that the asymmetry in the two coupled cells generally stabilizes the antiphase mode [16].

There have been many theoretical investigations on coupled oscillators [17–28]. Tyson and Kauffman studied the in-phase and antiphase modes in two coupled Brusselator models [17]. Baesens *et al.* [28] studied the behavior of three coupled oscillators and found four kinds of modes: full mode-locking, partially mode-locking, and incommensurate and toroidal chaos. Daido [24,25] and Shimizu and co-workers [26,27] studied the behaviors of interacting oscillators from the view point of the phase dynamics and showed that the frustration plays an important role in the synchronization among the three coupled oscillators.

It is natural to say that in biology the conjunctions among synapses and the shape and volume of cells are inherently asymmetric. So far, though many studies of synchronization have been studied in theory and experiment, the effects of asymmetry in coupling are still not revealed in detail. Furthermore, the frustration effect has not been studied well in an experimental system. Under these circumstances, we have found various modes in nonlinear oscillators by changing the symmetry of the coupling in actual experiments. To investigate the frustration effect, three coupled cells arranged in a triangular form have been chosen, since this is the simplest system capable of exhibiting frustration. We will focus our interest on the synchronization of three coupled oscillators as a function of the symmetry of coupling. We used the BZ reaction as the nonlinear oscillator. The coupling in

 

the BZ reaction among CSTR's was performed by using peristaltic pumps to control the coupling strength. Asymmetric coupling has been achieved to pump the mass flow among three reactors with different volumes. We have also attempted to interpret the experimental results in analogy with the coupled spin system [18,19,21–27].

Here, we would like to discuss the other physical meaning of volume deference in relation to the asymmetry of coupling. We describe two coupled cells as an example. Two coupled cells can be interpreted by the following equations:

$$\frac{dX_1}{dt}=F(X_1)+\frac{\rho}{R_1}(X_2-X_1)+\frac{1}{C_1}(X_1^0-X_1)\ , \quad (1)$$

$$\frac{dX_2}{dt}=F(X_2)+\frac{\rho}{R_2}(X_1-X_2)+\frac{1}{C_2}(X_2^0-X_2)\ . \quad (2)$$

$X=(u_1, u_2, u_3, \ldots, u_n)$, where $u_n$ is the concentrations of $n$th species in a CSTR, $\rho$ is the flow rate between the reactors, $R$ is the volume of CSTR, and $C$ ($=R/\tau$, $\tau$ is the flow rate of reactant solution applied from reservoirs into a CSTR) is a characteristic time, corresponding to the residence time without coupling. The $F(X)$ term means the appropriate nonlinear equation including the autocatalytic process, e.g., Brusselator, Oreganator, and Bonhoeffer–van der Pol equation. The suffix denotes each CSTR. $X^0=(u_1^0,u_2^0,\ldots,u_n^0)$, where $u_n^0$ is the concentrations of the $n$th species fed into a CSTR. From those equations, it is evident that the asymmetry due to the difference in CSTR volume is equivalent to the asymmetry in the mutual coupling strengths between CSTR's with the same volume. In the experiment, it is not desirable to achieve the asymmetry by changing the mutual pumping rates between CSTR's, since it changes the other important conditions, such as the net residence time after coupling as a combined effect of outlet flow and exchange flow, period of oscillator, etc. Therefore, in the present experiment, we have adopted the volume asymmetry to realize the asymmetric coupling.

## II. MATERIALS AND METHODS

The BZ reaction consisting of organic substrate, cerium ion, bromate, and sulfuric acid was studied to observe the synchronized modes in the coupled oscillators. The following materials were used without further purification: malonic acid, $Ce(SO_4)_2(NH_4)_4SO_4\cdot 2H_2O$, $KBrO_3$ (Katayama Chemical Industries Corporation, Ltd.), and $H_2SO_4$ (Wako Pure Chemical Industries, Ltd.). Two kinds of reactant solutions were made with 1.5$M$ $H_2SO_4$: one contained cerium and malonic acid, the other contained bromate. Each CSTR had two feedstreams, and the concentrations of all feedstream species were the same in the three CSTR's. If not otherwise stated, they were $[BrO_3^-]=5.0$ m$M$, [Ce IV]$=1.0$ m$M$, and [malonic acid]$=16$ m$M$, after mixing the reactant solutions in the CSTR's.

The experimental setup of the three coupled CSTR's and the detailed design of each CSTR are schematically shown in Figs. 1(a) and 1(b), respectively. The three CSTR's were arranged in a triangular manner and were connected to each other. The CSTR'S were made of Pyrex and the water jacket of Plexiglas. Each CSTR had four small inlets at the bottom: two were used for the reactant solutions from the reservoirs and the two others for the coupling with the neighboring CSTR's. Magnetic stirring was maintained sufficiently fast for the oscillatory period not to depend on stirring rate. The reacting solution was overflown through a hole in the top of each CSTR, and was removed by an aspirator. The hole also facilitated the escape of gas bubbles, such as carbon dioxide, the degradation products of malonic acid. The temperature of the CSTR's was kept at 49±0.1 °C by water circulation through the jacket pumped from a constant temperature bath. The CSTR's were mutually connected by two silicone tubes, 20 cm in length, and 1 or 2 mm in inner diameter, depending on the flow rate. The flow rates between CSTR's were controlled by peristaltic pumps, and were kept identical in both directions. All the flow rates through the connecting tubes were adjusted

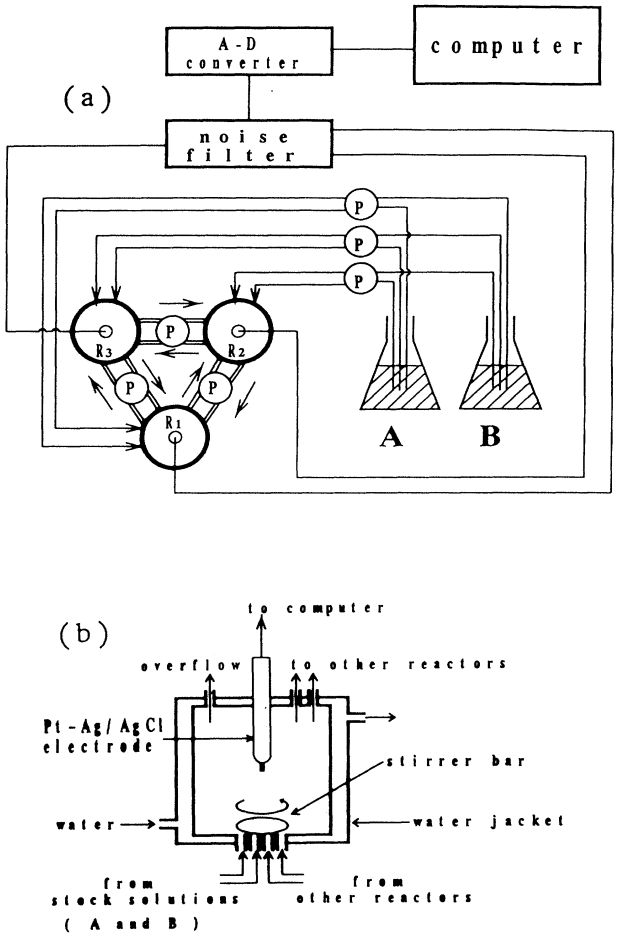


FIG. 1. (a) Experimental setup for the three coupled cells. $P$: peristaltic pump, $R_1$, $R_2$, and $R_3$: CSTR's, $A$: malonic acid and Ce IV in $H_2SO_4$; $B$: $KBrO_3$ in $H_2SO_4$. (b) Schematic representation of a CSTR.

as the same throughout a single experimental run. For the experiment with symmetric coupling, the three CSTR's had an active volume with $R_1=R_2=R_3=7.5$ ml. As for the experiment with asymmetric coupling, the CSTR's were designed so as to have different volumes with $R_1=19.0$ ml, $R_2=11.0$ ml and $R_3=7.5$ ml. The experimental procedure was as follows. The CSTR's were initially filled with the reactant solutions. After the oscillations began, the flow of the reactant solutions was started. When the oscillations in three CSTR's became stationary after 1–2 h of continuous pumping, the coupling experiments were started with desired coupling strength. The redox potential was measured as the electrical potential between a Ag-AgCl reference electrode and a platinum electrode inserted into the top of each CSTR. Though the platinum electrode detects somewhat complicated potential depending not only on the ratio of oxidized and reduced forms of cerium but also on some oxybromine compounds, the potential is mainly attributable to cerium, since the concentration of the cerium ion is much higher than that of the oxybromine compounds [9]. The time trace data for the redox potentials were sampled at 1-s intervals, and stored on a personal computer NEC-PC9801 through a voltage follower, a noise filter, and an $A-D$ converter (Contec, Ltd.).

We have confirmed, in the experiment on the coupled oscillators, that the time delay due to mass transfer of the reacting solution through the connecting tube had a negligible effect on the mode of the synchronization.

## III. RESULTS AND DISCUSSION

### A. Three coupled cells

In the three coupled cells, the change of the interference mode was studied as a function of the coupling strength for both the symmetric and asymmetric couplings. The natural periods, without coupling, were adjusted to 120±10 s in both the symmetric and asymmetric couplings. The periods of the three chemical oscillators were adjusted to show similar periods, wave forms, and amplitudes, in order to avoid the generalization of complicated modes of synchronization [4,9]. The results of the synchronization for the three coupled cells will be described in two different parts, the symmetric coupling and the asymmetric coupling.

#### *1. Symmetric coupling*

In the case of symmetric coupling, an increase of coupling strength was accompanied by the appearance of a quasiperiodic state or a biperiodic mode, a phase-death mode, and two kinds of synchronized modes. In Fig. 2, a quasiperiodic state or a biperiodic mode, a phase-death mode, and two kinds of synchronized modes are shown as the time traces of the redox potential. The residence times for three CSTR's were adjusted to 16.3 min. Figure 3 indicates the three-dimensional view of attractors for the experiment given in Fig. 2. The coupling strength, $\rho$ (ml/min), increases in the order of (a) < (b) < (c) < (d) in

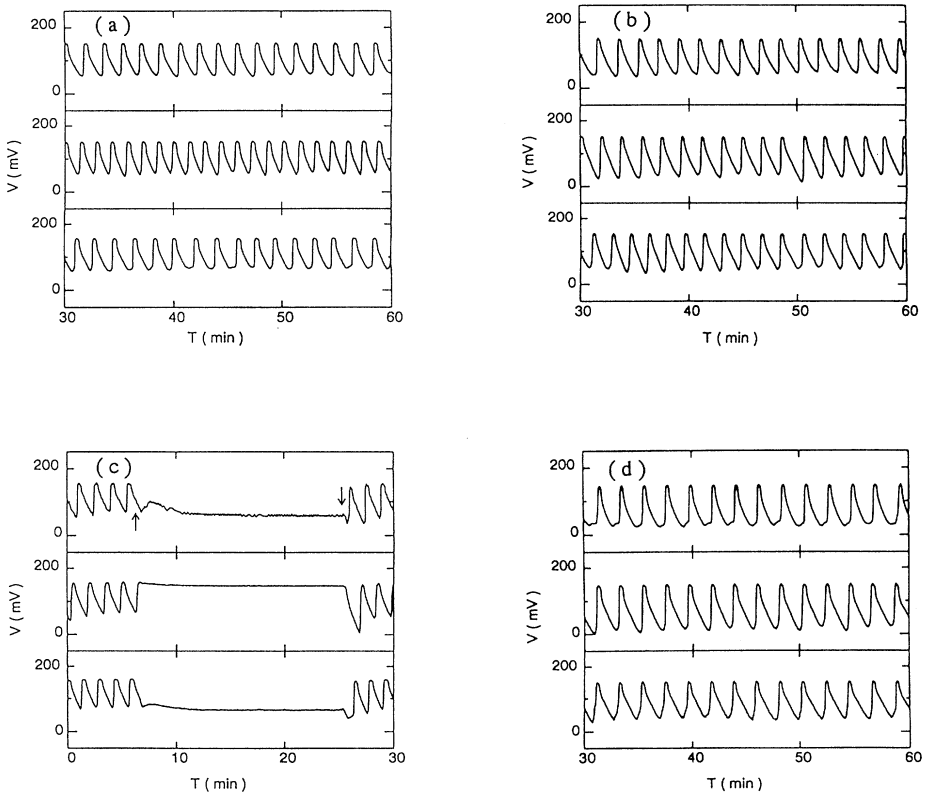


FIG. 2. Experimental traces of redox potential for the symmetric three coupled oscillators from 0 to 30 min or from 30 to 60 min after the start of coupling. The CSTR volume is $R_1=R_2=R_3=7.5$ ml. The bottom trace is the redox potential $V_1$ in $R_1$. The middle trace is $V_2$ in $R_2$. The top trace is $V_3$ in $R_3$. (a) Quasiperiodic state of biperiodic mode: the coupling flow rate among three CSTR's was 0.360 ml/min; (b) three-phase mode: the coupling flow rate was 1.40 ml/min. This mode appears only as a transient and shows fluctuation between the bistable modes with the opposite phase difference. (c) All-death mode (ADS): the coupling flow rate was 2.70 ml/min. The upward arrow and the downward arrow show the points of the start and end of coupling, respectively. (d) All-in-phase mode: the coupling flow rate was 3.40 ml/min.

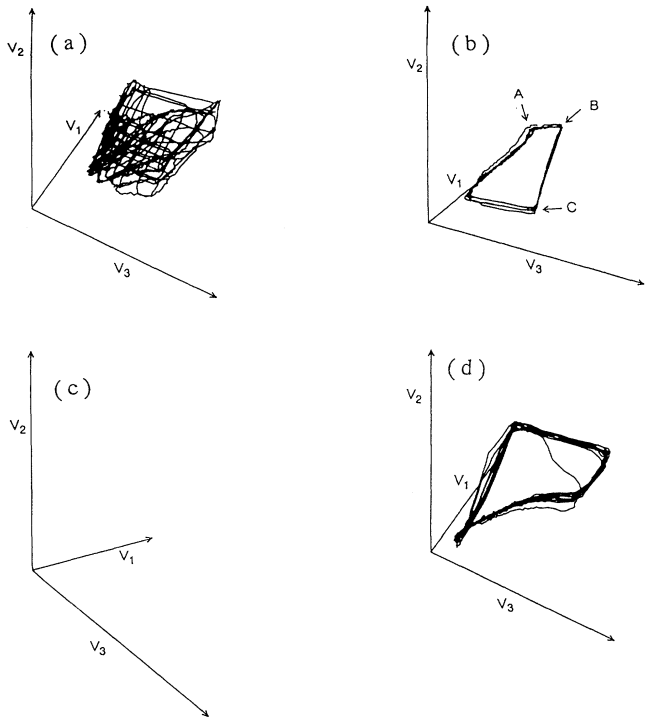


FIG. 3. Three-dimensional view of attractors for the results in Fig. 2. (a) Quasiperiodic state or biperiodic mode; (b) "transient" three-phase mode, the three-dimensional view of attractor is given for the period between 30 and 40 min after the start of coupling. The marks, *A*, *B*, and *C*, indicate the maximum redox potential of $R_1$, $R_2$, and $R_3$, respectively. (c) All-death mode (ADS); (d) all-in-phase mode.

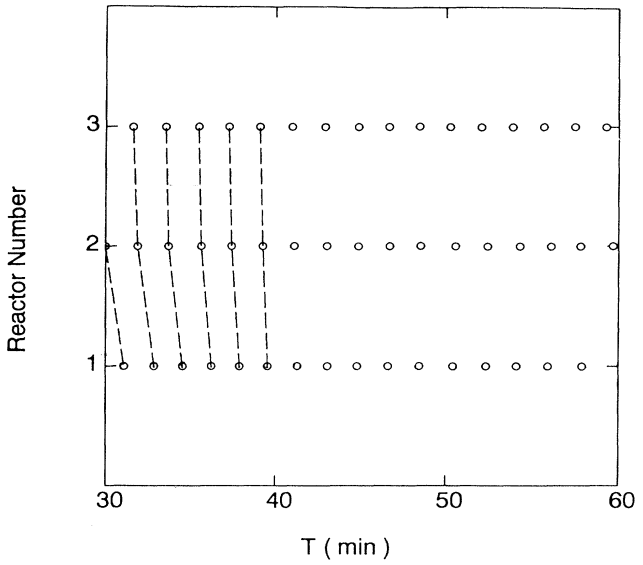


FIG. 4. "Transient" three-phase mode in the three coupled oscillators. The open circles indicate the points of the maximum redox potential.

Figs. 2 and 3.

When the coupling strength was less than $\rho=1.30$ ml/min, a quasiperiodic state or a biperiodic mode was observed [Figs. 2(a) and 3(a)]. In this case, the period in $R_2$ was $100\pm5$ s, being smaller than the intrinsic period. This is in contrast with a previous study [9], where the period in the quasiperiodic state or biperiodic mode remains essentially constant. The periods in $R_1$ and $R_3$ showed no apparent change. The quasiperiodic state or biperiodic mode means that when three CSTR's are coupled they are not entrained into a common period. As shown in Fig. 3(a), the three-dimensional view of the trace of attractor for the quasiperiodic state or biperiodic mode shows a torus without forming a closed cycle.

When $\rho$ was between 1.30 and 1.60 ml/min, the three-phase mode appeared transiently [Figs. 2(b) and 3(b)], where the phase differences among three coupled oscillators were found to be nearly $2\pi/3$ and $4\pi/3$. Figure 4 shows points when the oscillators exhibit the maximum redox potential. The open circles indicated for CSTR's, $R_1$, $R_2$, and $R_3$, in Fig. 4 correspond to the marks, *A*, *B*, and *C*, in Fig. 3(b), respectively. When the oscillators were synchronized into this mode, the periods of three oscillations were $120\pm10$ s. In Figs. 2(b) and 4, the phase differences among the three oscillators were nearly $2\pi/3$ each other from 30 to 40 min and were inverted from 50 to 58 min after the start of coupling. It is apparent that the three-phase mode is bistable and they spontaneously fluctuate to each other. In the symmetric coupling, various modes appear under the same conditions and the three-phase mode does not seem so stable. However, the three-dimensional view of attractor given in Fig. 3(b) clearly indicates that the oscillators are entrained into a three-phase mode at least for 30–40 min during the experiment. We are believing that such a phenomenon is quite interesting as a self-wandering phenomenon among various modes. In the three-phase mode [12,18,24], the phase differences among three oscillators are $2\pi/3$, where the phase wave rotates around the triangle connection of the CSTR's. The three-phase mode is, thus, bistable with $2\pi/3$ and $-2\pi/3$ modes in its intrinsic nature. In the actual experiment, the phase differences in the three-phase mode were not just $2\pi/3$ or $-2\pi/3$, because of several unavoidable experimental factors, such as inhomogeneities in a CSTR [29], different response of individual electrodes, etc.

We call ADS the all-death mode in the case of the symmetric coupling as in Figs. 2(c) and 3(c). As shown in Fig. 3(c), the ADS is a stable fixed point in the three-dimensional view of attractor. The ADS was observed for the range between $\rho=1.50$ and 3.40 ml/min. In this mode, one CSTR was fixed at a high redox potential, while the two others were at low redox potentials [Fig. 2(c)]. It has been confirmed from several experimental runs that there is equal probability for each oscillator to be fixed at the high potential. Figures 2(c) and 3(c) indicate the case when $R_2$ shows the high potential. Figure 3(c) shows that the attractor is a fixed point in the three-dimensional view of attractor, though the point is somewhat blurred due to relaxation process from the oscillating state.

Further increase of the coupling strength induced the bifurcation from ADS to the all-in-phase mode [Figs. 2(d) and 3(d)]. The all-in-phase mode appeared when the coupling strength, $\rho$, was more than 3.00 ml/min. In the all-in-phase mode, the periods and phases in the three coupled CSTR's were equal, and the periods were $120\pm10$ s. It is natural that the all-in-phase mode is generated when the coupling is sufficiently strong. At the high limit of the coupling strength, the concentrations of all species for the reacting solution become the same in the three coupled CSTR's. The homogeneity produces, as a result, a single, three-lobed CSTR and, thus, the all-in-phase mode appears.

Although, in our experiment, the attractors do not trace a single closed line in Figs. 3(b) and 3(d) or a fixed point in Fig. 3(c) from the mathematical point of view, we would like to classify these different modes using the terms three-phase mode, ADS, and all-in-phase mode. The phase diagram of the ADS and two kinds of synchronized modes for the symmetric coupling is shown in Fig. 5. There were bistable regions where both the three-phase mode and the ADS or both the ADS and the all-in-phase mode were observed, depending on the initial conditions or the pathway of the parameter change.

### 2. *Asymmetric coupling*

In the case of the asymmetric coupling, a quasiperiodic state or a biperiodic mode, a phase-death mode, and four kinds of synchronized modes appeared depending on the coupling strength. In Fig. 6, a quasiperiodic state or a biperiodic mode, a phase-death mode, and four kinds of synchronized modes are shown as the time traces of the redox potential. The residence times of the three CSTR's were as follows: $R_1$ had 20.2 min, $R_2$ had 18.3 min, and $R_3$ had 16.3 min. Figure 7 shows the three-dimensional view of attractors for Fig. 6. The coupling flow rate, $\rho$, successively increased in the order of (a) < (b) < (c) < (d) < (e) < (f) in Figs. 6 and 7.

The quasiperiodic state or biperiodic mode was observed for the range with less than $\rho=1.02$ ml/min [Figs. 6(a) and 7(a)]. In the quasiperiodic state or biperiodic mode, the coupled periods in three CSTR's did not change. Similar to the symmetric coupling, the trace of the three-dimensional attractor for the quasiperiodic state or biperiodic mode constitutes a torus.

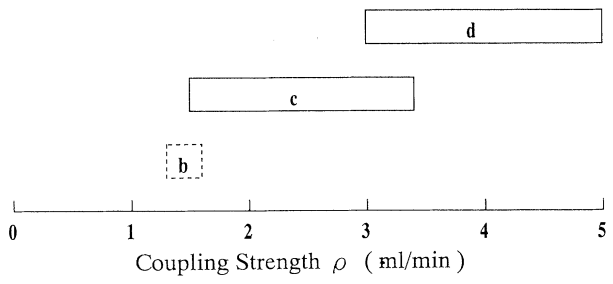


FIG. 5. Phase diagram for ADS and two kinds of synchronized modes in the symmetric three coupled oscillators as a function of the coupling strength $\rho$; box *b*, "transient" three-phase mode; *c*, all-death mode (ADS); *d*, all-in-phase mode.

The three-phase mode occurred for the range between $\rho=1.02$ and 1.54 ml/min [Figs. 6(b) and 7(b)]. In Fig. 8, the open circles indicate the times with the maximum redox potential. The open circle marked for CSTR's, $R_1$, $R_2$, and $R_3$ in Fig. 8 correspond to the marks, *A*, *B*, and *C* in Fig. 7(b), respectively. The *B* traces in Fig. 7(b) show two different circles, suggesting that there is self-switching between the two modes. In the present experimental condition, the two modes exhibited spontaneous changes at 10–15-min intervals. The periods in three CSTR's remained almost constant. The squarelike shape of the attractor for the three-phase mode in the asymmetric coupling case is similar to that of the symmetric coupling. On the other hand, the three-phase mode in the asymmetric coupling is apparently different from that in the symmetric coupling. In the asymmetric coupling, the rotational direction of the phase wave always followed the order

$$R_3\ (7.5\ \text{ml}) \rightarrow R_2\ (11.0\ \text{ml}) \rightarrow R_1\ (19.0\ \text{ml}).$$

This means that it is possible to control the rotational direction of phase wave as shown in Fig. 9. Figures 6(b), 7(b), and 8 show that the phase differences are $2\pi/3$ of each other. On the other hand, the phase differences become $-2\pi/3$ of each other when the arrangement of $R_2$ and $R_3$ is mutually changed (Fig. 9). It is clear that the bi- stable three-phase modes become monostable due to the asymmetry of the coupling. The rotational direction is determined as follows. When the large volume CSTR fires or shows the maximum redox potential for the first time, the small volume CSTR is affected more than the middle volume CSTR. The small volume CSTR, thus, fires or takes the maximum potential. Then, both the large and small volume CSTR's affect, as a result, the middle volume CSTR. This process is repeated again and again, generating the monostable three-phase mode.

For the range of $\rho=1.30$ to 3.60 ml/min, the mode as in Fig. 6(c) appeared. We call this a death in-phase mode. In this mode, the periods of $R_1$ and $R_2$ were $120\pm10$ s, while $R_3$ always settled in the death mode. As shown in Fig. 7(c), the oscillation of the synchronized mode is observed only on the $V_1$-$V_2$ plane.

For the range $\rho=1.40-1.92$ ml/min, the mode as in Fig. 6(d) was observed. We call this mode a death anti-phase mode. In this mode, similar to the death in-phase mode, the phase-death mode always took place in $R_3$. The periods of $R_1$ and $R_2$ were lengthened to 150–200 s. Figure 7(d) shows the three-dimensional view of attractor. The oscillation of the synchronized mode is observed only on the $V_1$-$V_2$ plane.

In the range $\rho=350-4.70$ ml/min, the mode of Fig. 6(e) was observed. We call this mode an all-death mode in the asymmetric coupling (ADA). In the ADA, the redox potentials of the all-death mode in three CSTR's were separated into three states: the small CSTR always had a high redox potential, the middle CSTR always had a middle redox potential, and the large CSTR always had a low redox potential. This is quite different from the stochastic nature of the tristable death modes in the symmetric coupling. Thus, the asymmetric coupling breaks

the degeneracy in the death mode, and generates new multistable modes. Figure 7(e) shows that the ADA has a stable fix point.

When the coupling strength was greater than $\rho=2.70$ ml/min, the all-in-phase mode appeared as shown in Figs. 6(f) and 7(f). The three-dimensional view of attractor is similar to that of the symmetric coupling.

The phase diagram of the ADA and four kinds of synchronized modes is shown in Fig. 10, showing that there are bistable and tristable regions. We have found that the number of the synchronized modes in the asymmetric coupling increases compared to those in the symmetric coupling. It is also noted that the parameter space of the three-phase mode in the asymmetric coupling is greater than that in the symmetric coupling.

### B. Three coupled cells in comparison with the two coupled cells

In the three coupled cells, we have observed various modes, such as the quasiperiodic state or biperiodic mode, phase-death modes, and several kinds of synchronized modes, for both cases with the symmetric and asymmetric couplings. To obtain further insight into the dy-

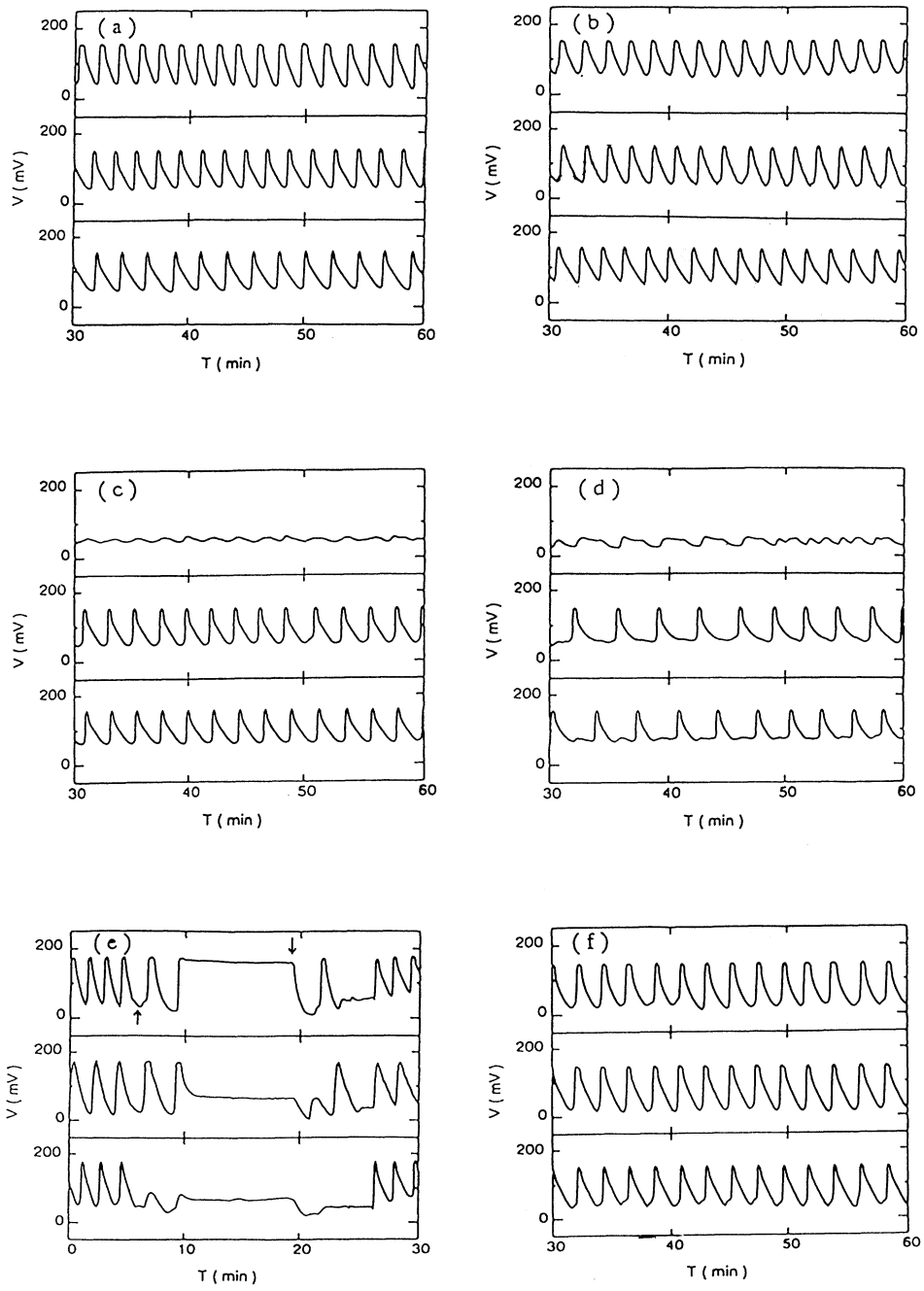


FIG. 6. Experimental traces of redox potential for the asymmetric three coupled oscillators from 0 to 30 min or from 30 to 60 min after the start of coupling. The CSTR volumes were $R_1=19.0$ ml, $R_2=11.0$ ml, and $R_3=7.5$ ml. The bottom trace is the redox potential $V_1$ in $R_1$. The middle trace is $V_2$ in $R_2$. The top trace is $V_3$ in $R_3$. (a) Quasiperiodic state or biperiodic mode: the coupling flow rate among the three CSTR's was 0.360 ml/min; (b) three-phase mode: the coupling flow rate was 1.15 ml/min; (c) death in-phase mode: the coupling flow rate was 1.92 ml/min; (d) death antiphase mode: the coupling flow rate was 1.66 ml/min; (e) all-death mode (ADA): the coupling flow rate as 4.10 ml/min. The upward arrow and the downward arrow show the points when the coupling starts and the coupling ends, respectively. (f) All-in-phase mode: the coupling flow rate was 4.75 ml/min.

namic stability in the three coupled oscillators, we studied the behavior of two coupled cells. In the two coupled cells, the experimental conditions were chosen similar to those of the three coupled cells. In the symmetric coupling, the two CSTR's had the active volume with $R_1=R_2=7.5$ ml. As for the asymmetric coupling, we have studied for three different sets of volumes, ($R_1$, $R_2$)=(7.5 ml, 11.0 ml), (7.5 ml, 19.0 ml) and (11.0 ml, 19.0 ml). For all of the experiments with the symmetric coupling and the asymmetric coupling, two kinds of 1:1 synchronized modes were observed: the antiphase mode (the phase difference, $\Delta\phi=\pi$) and the in-phase mode ($\Delta\phi=0$). The phase diagram in the two coupled cells is shown in Fig. 11. As the coupling strength increased, the synchronized mode changed from the antiphase mode into the in-phase mode. When the periods of uncoupled oscillators were 120±10 s, in these experiments, the periods of the antiphase mode were lengthened to 250±5 s, while the periods of the in-phase mode remained at 120±10 s. From Fig. 11, it is evident that the parameter space for the antiphase mode becomes greater with an increase of the asymmetry.

Then, we would like to discuss the stability in the three coupled cells based on the knowledge on the stability in the two coupled cells [18,19,21–27]. Let us begin with the following ordinary differential equation describing the phase dynamics:

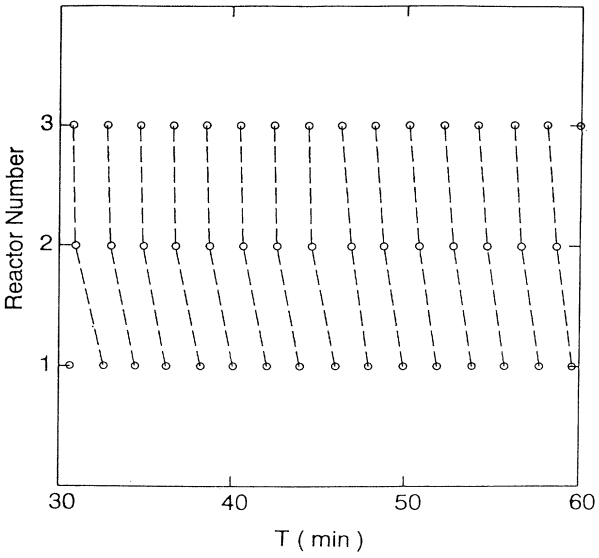


FIG. 8. A three-phase mode with the phase difference of $2\pi/3$, i.e., $\theta_2-\theta_3=\theta_1-\theta_2=2\pi/3$. The open circles indicate the points with the maximum redox potential.

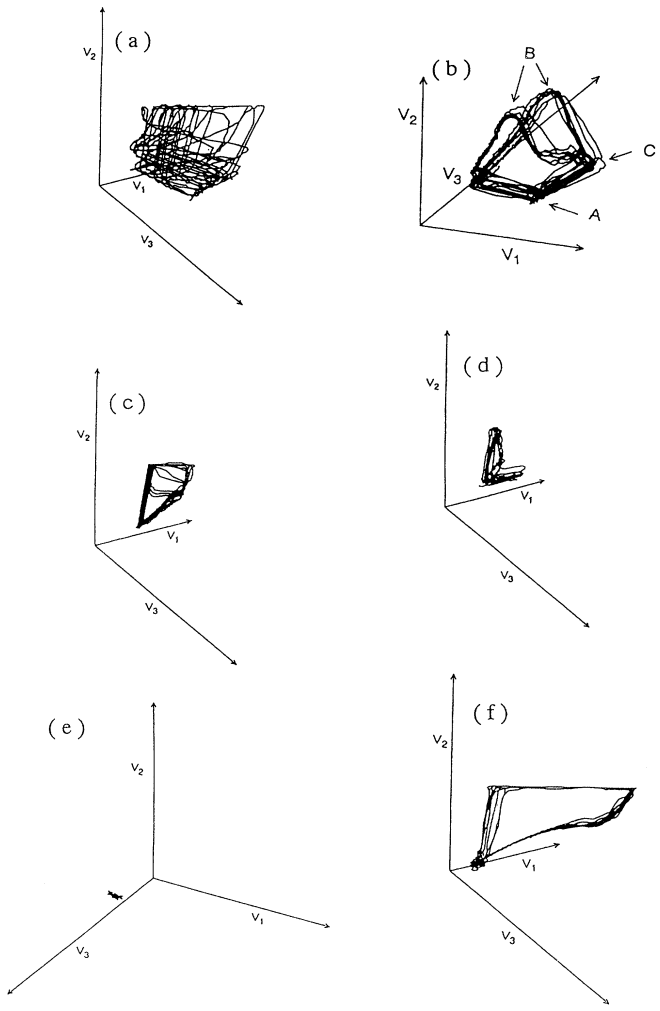


FIG. 7. Three-dimensional view of attractors for the results in Fig. 6. (a) Quasiperiodic state of biperiodic mode; (b) three-phase mode: the marks, *A*, *B*, and *C* indicate the maximum redox potential of $R_1$, $R_2$, and $R_3$, respectively; (c) death-in-phase mode; (d) death antiphase mode; (e) all-death mode (ADA); (d) all-in-phase mode.

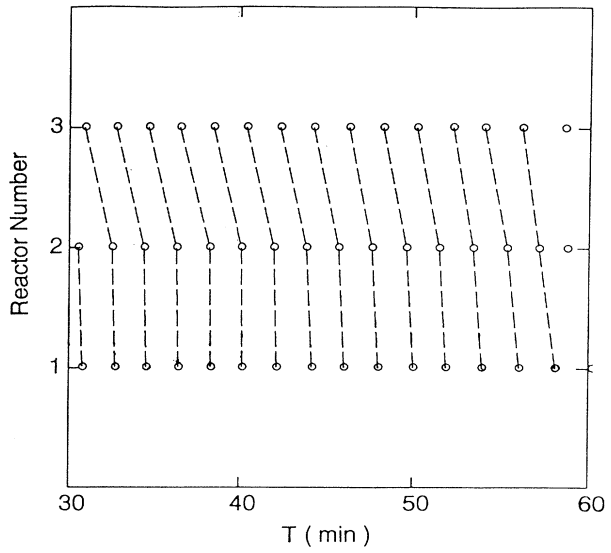


FIG. 9. The other three-phase mode with the phase difference of $-2\pi/3$, i.e., $\theta_2-\theta_3=\theta_1-\theta_2=-2\pi/3$. The open circles indicate the points of the maximum redox potential.

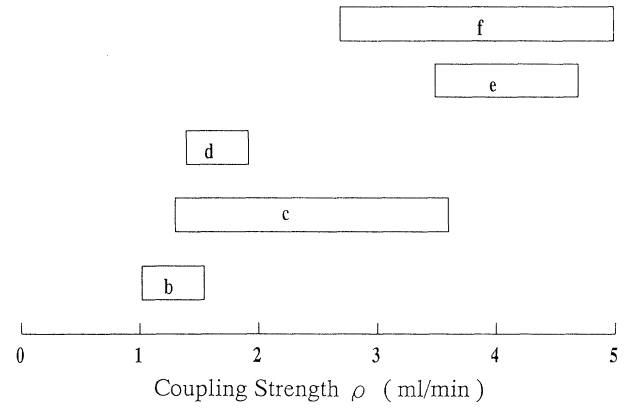


FIG. 10. Phase diagram for ADA and phase-locking modes in the asymmetric three coupled oscilaltors as a function of the coupling strength $\rho$: Box $b$, three-phase mode; $c$, death in-phase mode; $d$, death antiphase mode; $e$, all-death mode (ADA); $f$, all-in-phase mode.

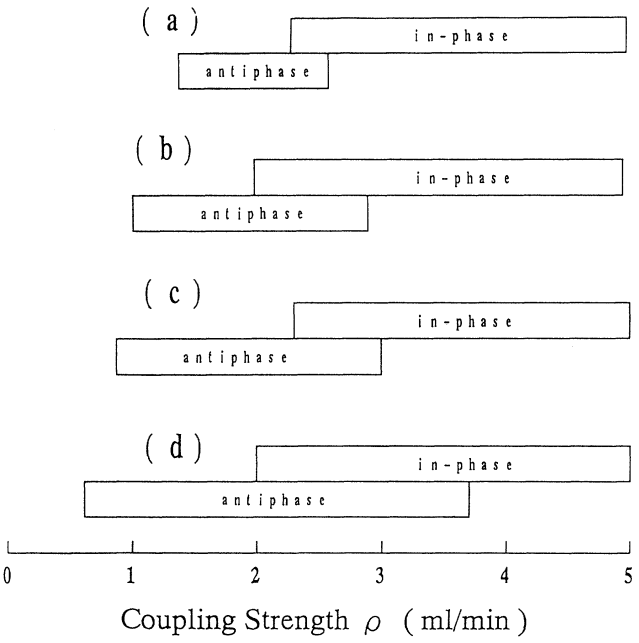


FIG. 11. Phase diagram for the synchronized modes in the two coupled oscillators as a function of the coupling strength $\rho$. (a) The volume was $R_1=R_2=7.5$ ml: the antiphase mode appeared for the range between $\rho=1.40$ and 2.60 ml/min. The in-phase mode was observed for $\rho>2.30$ ml/min. (b) The volumes were $R_1=7.5$ ml and $R_2=11.0$ ml: the antiphase mode appeared for the range between $\rho=1.02$ and 2.90 ml/min. The in-phase mode was observed for $\rho>2.6$ ml/min. (c) The volumes were $R_1=11.0$ ml and $R_2=19.0$ ml: the antiphase mode appeared for the range between $\rho=0.880$ and 3.00 ml/min. The in-phase mode was observed for $\rho>2.30$ ml/min. (d) The volumes were $R_1=7.5$ ml and $R_2=19.0$ ml: the antiphase mode appeared for the range between $\rho=0.620$ and 3.70 ml/min. The in-phase mode was observed for $\rho>2.00$ ml/min.

$$\frac{d\phi_i}{dt}=\omega_i-\sum_{\substack{j=1\\ j\neq i}}^{n}J_{ij}\sin(\phi_i-\phi_j), \tag{3}$$

where $\phi_i$ represents the phase of the $i$th oscillator with natural frequency $\omega_i$, and $J_{ij}$ is the interaction parameter between the $i$th and $j$th oscillators. For the two coupled oscillators, i.e., $n=2$, the following pair of equations is derived when $\omega_1=\omega_2=\omega$ and $J_{12}=J_{21}=J$:

$$\frac{d\phi_1}{dt}=\omega-J\sin(\phi_1-\phi_2), \tag{4}$$

$$\frac{d\phi_2}{dt}=\omega-J\sin(\phi_2-\phi_1). \tag{5}$$

The phase difference, $\Psi_{12}=\phi_1-\phi_2$, has two stationary values, 0 and $\pi$, where the former is stable for $J>0$, i.e., the in-phase mode, and the latter is stable for $J<0$, i.e., antiphase mode. It is noted that there is an analogy between the modes of coupled oscillators and the states of coupled Ising spins. Thus, the sign of $J$ determines whether the interaction is a ferromagnetic interaction or an antiferromagnetic one in the corresponding coupled-spin system. Then, for the three coupled cells, i.e., $n=3$, we may define the frustration function $\Psi$ [24] by

$$\Psi=(1-\tau_{12}\tau_{23}\tau_{31})/2, \tag{6}$$

where $\tau_{ij}=\mathrm{sgn}J_{ij}$. $\Psi=1$ indicates the existence of frustration and $\Psi=0$ indicates its absence. In a triangular form, $\Psi=1$ when one of three $J_{ij}$'s is negative and the others are positive or when all $J_{ij}$ are negative.

As a next step, we would like to discuss the relationship between the two coupled cells and the three coupled cells. From the phase diagrams, Figs. 5, 10, and 11, it is clear that, in both the symmetric and asymmetric couplings, the three-phase mode appears for the parameter area where all of the pairs of the oscillators show the antiphase mode, $\Psi=1$. It is also clear that the three-phase mode appears when the coupling strength is relatively weak. Therefore, it is considered that the appearance of the three-phase mode comes from a compensation effect for the weakly frustrated oscillators with slight mutual phase shifts between the coupled oscillators.

We have also found that the two kinds of synchronized modes in the asymmetric coupling, death in-phase mode and death antiphase mode, were induced by the frustration. The two kinds of synchronized modes appeared in a stronger coupling range than the three-phase mode. In this case, the frustration is stronger than that of the three-phase mode and cannot be compensated for by the mutual phase change. It is considered that the frustration always brought about the phase-death mode in the smallest volume CSTR.

It is interesting to note that the parameter area of the all-death mode, ADS and ADA, is rather great, in contrast to the lower stability of the death mode in two coupled oscillators. This suggests that the strong frustration may induce the all-death mode.

Let us compare the death mode in the two coupled cells with those in the three coupled cells. Figure 12 shows the time trace of the phase-death mode in the two

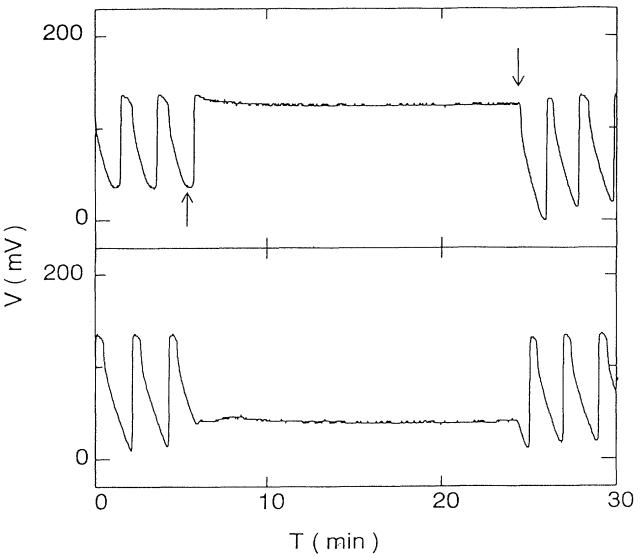


FIG. 12. Experimental traces of the phase-death mode for the two coupled cells in the asymmetric coupling. The experimental conditions for phase death mode in two coupled cells were as follows. In the case of the symmetric coupling, the reactor volume was $R_1=R_2=7.5$ ml and the residence time was 16.3 min. In the case of the asymmetric coupling, the reactor volumes were $R_1=19.0$ ml and $R_2=7.5$ ml, and the residence times were 20.3 and 16.3 min, respectively. The initial concentrations in the two reactors, that is, the concentrations after mixing the reactant solutions, were $[BrO_3^-]=10$ m$M$, [Ce IV]$=1.0$ m$M$, and [malonic acid]$=32$ m$M$. The temperature was kept at 37 °C. The bottom trace is the redox potential $V_1$ in $R_1$. The top trace is $V_2$ in $R_2$. The coupling flow rate was 4.00 ml/min. The upward arrow and the downward arrow show the points when the coupling starts and the coupling ends, respectively.

coupled cells. We have found the common characters as follows.

(i) *Symmetric coupling.* One CSTR exhibits a high redox potential and the other exhibits a low potential; the probability to be the high potential for each CSTR is stochastic.

(ii) *Asymmetric coupling.* The high and low redox potentials are observed depending on the relative size of the CSTR volume. The small volume reactor always assumes the high and the large volume reactor the low redox potential.

These results may provide important suggestions as to the behaviors of interacting nonlinear oscillators.

### C. Synchronized mode of nonlinear oscillator in relation to the $XY$ spin system

In the preceding section, the frustration in coupled oscillator was discussed in relation to that in the Ising spin system. It has been shown that in the three coupled cells, the frustration causes the change from the Ising spin system into the $XY$ spin system, taking into account the effects of the phase shift. Kuramoto and co-workers [18,19,21–23], Shimizu and co-workers [26,27], and Daido [24,25] studied synchronization of interacting dissipative nonlinear oscillators from the theoretical point of view. They considered the similarity of the nonlinear oscillator with the $XY$ spin and explained some aspects of synchronization. They have, however, studied only the oscillatory state. In our experiment, ADA, ADS, death in-phase mode, and death antiphase mode appear. Thus, we would like to discuss further both the oscillatory state and the death state using the following equation for oscillators, which corresponds to Hamiltonian in the $XY$ spin system [30]:

$$G=-\sum_{\substack{i,j\\ i\neq j}}\tau_{ij}\tilde{J}_{ij}S_iS_j, \tag{7}$$

where $|J_{ij}|=\tilde{J}_{ij}$, $\tau_{ij}=\mathrm{sgn}J_{ij}$ and $S$ has the meaning of the synchronized dynamical phase of nonlinear oscillator. $S$ may be defined as follows.

(i) If the oscillators oscillate, $S=\cos(\omega t+\alpha)$, where we take an approximation that $S$ is given only with fundamental frequency of nonlinear oscillator [18,19,21–27] and $\alpha$ is the difference of phase angle between oscillators.

(ii) If the oscillators do not oscillate, $S=\pm1$ and 0, where $+1$, $-1$, and 0 mean that oscillator is resting in the up state, the down state, and the middle state, respectively.

TABLE I. $\bar{G}$ values calculated from Eq. (8) for the case $\tau_1=\tau_2=\tau_3=-1$.

| | Values of $S$ | $\bar{G}$ |
|---|---|---|
| Three-phase mode | $S_1=\cos\omega t$, $S_2=\cos(\omega t+2\pi/3)$, $S_3=\cos(\omega t+4\pi/3)$ | $-\frac{3J}{4}$ |
| Death in-phase mode | $S_1=-1$, $S_2=\cos\omega t$, $S_3=\cos\omega t$ | $\frac{J}{2}$ |
| Death antiphase mode | $S_1=-1$, $S_2=\cos\omega t$, $S_3=\cos(\omega t+\pi)$ | $-\frac{J}{2}$ |
| ADS[a] | $S_1=-1$, $S_2=-1$, $S_3=+1$ | $-J$ |
| ADA[b] | $S_1=-1$, $S_2=0$, $S_3=+1$ | $-J$ |
| All-in-phase mode | $S_1=\cos\omega t$, $S_2=\cos\omega t$, $S_3=\cos\omega t$ | $\frac{3J}{2}$ |
| Two in-phase frustrated state | $S_1=\cos\omega t$, $S_2=\cos\omega t$, $S_3=\cos(\omega t+\pi)$ | $-\frac{J}{2}$ |

[a]All-death mode in the symmetric coupling.
[b]All-death mode in the asymmetric coupling.

TABLE II. Difference between the symmetric coupling and the asymmetric coupling in the three-coupled system.

| | Symmetric coupling | Asymmetric coupling |
|---|---|---|
| Number of stable modes | 3 (see Fig. 5) | 5 (see Fig. 10) |
| Stability of the three-phase mode | bistability[a] | two kinds of monostabilities |
| Stability of the death mode | 2 stable states (stochastic) | 3 stable states (deterministic) |
| Mode caused by frustration | three-phase mode ADS[b] | three-phase mode death in-phase mode death antiphase mode ADA[c] |

[a]In our experiment, the three-phase mode appears as transient and the bistable modes with opposite phase difference switch each other spontaneously (see Fig. 4).
[b]All-death mode in the symmetric coupling.
[c]All-death mode in the asymmetric coupling.

Thus, the $G$ values averaged over one period ($=T$) may be calculated for the synchronized modes.

$$\bar{G}=-\frac{J}{T}\int_{t}^{t+T}(\tau_{12}S_1S_2+\tau_{23}S_2S_3+\tau_{31}S_3S_1)dt, \tag{8}$$

where $\tilde{J}_{ij}=J$ for all $(i,j)$, it is assumed that $J$ does not change in the antiphase mode and the in-phase mode and $\bar{G}$ values remain constant between the symmetric and asymmetric couplings. $\bar{G}$ values for the case $\tau_1=\tau_2=\tau_3=-1$ are listed in Table I. We also calculated for a frustrated state ($\bar{G}=-J/2$), where $\tau_1=\tau_2=+1$ and $\tau_3=-1$, $S_1=S_2=S_3=\cos\omega t$. These results indicate that $\bar{G}$ values in the three-phase mode, ADS, and ADA are smaller than those of the frustrated state without any phase shift. The $\bar{G}$ value may correspond to the time-averaged stability of the $XY$ spin system. Consequently, these modes may be more stable than the frustrated state with the triangular connections. On the other hand, $\bar{G}$ values of the death antiphase mode and the death in-phase mode are smaller than those of the frustrated state with the all-in-phase mode (Table I). These considerations may indicate that the death antiphase mode and the death in-phase mode also appear for the coupled oscillators with triangular connections. However, the $\bar{G}$ value of two in-phase frustrated state is smaller than that of the death in-phase mode and is the same as that of the death antiphase mode. In this case, it is considered that the asymmetry of connection plays an essential role in determining the stability of the frustrated state.

Four coupled oscillators arranged in a cyclic form may also be discussed using $\bar{G}$ value. In an all-in-phase mode, the $\bar{G}$ value is $-2J$, where $\tau_1=\tau_2=\tau_3=\tau_4=+1$, $S_1=S_2=S_3=S_4=\cos\omega t$. In an all antiphase mode, the $\bar{G}$ value is $-2J$, where $\tau_1=\tau_2=\tau_3=\tau_4=-1$, $S_1=S_3=\cos\omega t$, $S_2=S_4=\cos(\omega t+\pi)$. The $\bar{G}$ value of an all-death mode is 0, where $\tau_1=\tau_2=\tau_3=\tau_4=-1$, $S_1=S_2=S_3=-1$, $S_4=+1$. The $\bar{G}$ values are smaller than that of a frustrated state ($\bar{G}=2J$), where $\tau_1=\tau_2=\tau_3=\tau_4=-1$, $S_1=S_2=S_3=S_4=\cos\omega t$. Then, the all antiphase mode and all-death mode may tend to appear, when $\tau_1=\tau_2=\tau_3=\tau_4=-1$. In this way, it may be possible to anticipate the coupling modes, using the $\bar{G}$ value for the case of more than five coupled oscillators and for more complicated coupled oscillators, e.g., a neural network. The discussion of the $\bar{G}$ value may explain some important aspects of the dynamic mode, especially for the phase dynamics, in frustrated oscillator. Theoretical analysis including the effect of amplitude modulation is now underway in our research group.

## IV. CONCLUSION

We have observed a variety of modes for three coupled oscillators. We have found that the behavior of an oscillator with the asymmetric coupling is quite different from that with the symmetric coupling, and that the frustration plays an important role in the coupled oscillators. The results are listed in Table II. It is evident that the asymmetry brings about new multistable modes, and changes the stability of the three-phase mode from bistable into monostable. Besides the BZ reaction, it is expected that these trends are general in the coupling among nonlinear oscillators. These results may be useful to predict the behavior of interacting nonlinear oscillators with more complicated connections.

## ACKNOWLEDGMENTS

The authors are indebted to Professor M. Menzinger (University of Toronto) for his critical comments and corrections of manuscript. This work was partly supported by a Grant-in-Aid for Scientific Research to K.Y. from the Ministry of Education, Science and Culture of Japan. The authors thank Professor I. Hanazaki (IMS) and Professor S. Ikeda (Nagoya University) for their helpful support, and are grateful to Associate Professor M. Sasai (Nagoya University), Professor H. Nagashima (Shizuoka University), and Dr. J. Gorecki (IMS) for critical discussion and comments.

*To whom correspondence should be addressed.

[1] A. T. Winfree, *The Geometry of Biological Time* (Springer-Verlag, New York, 1980).
[2] R. J. Field, E. Körös, and R. M. Noyes, J. Am. Chem. Soc. **94**, 8649 (1972).
[3] R. J. Field and R. M. Noyes, J. Chem. Phys. **60**, 1877 (1974).
[4] M. Marek and I. Stuchl, Biophys. Chem. **3**, 241 (1975).
[5] H. Fujii and Y. Sawada, J. Chem. Phys. **69**, 3830 (1978).
[6] K. Nakajima and Y. Sawada, J. Chem. Phys. **72**, 2231 (1980).
[7] K. Bar-Eli and S. Reuveni, J. Phys. Chem. **89**, 1329 (1985).
[8] M. T. Beck and I. P. Nagy, J. Phys. Chem. **93**, 7755 (1985).
[9] M. F. Crowley and R. J. Field, J. Phys. Chem. **90**, 1907 (1986).
[10] M. Boukalouch, J. Elezgaray, A. Arneodo, J. Boissonade, and P. De Kepper, J. Phys. Chem. **91**, 5843 (1987).
[11] M. F. Crowley and I. R. Epstein, J. Phys. Chem. **93**, 2496 (1989).
[12] K. Yoshikawa, K. Fukunaga, and H. Kawakami, Chem. Phys. Lett. **174**, 203 (1990).
[13] C. M. Marcus, F. R. Waugh, and R. M. Westervelt, Physica D **51**, 234 (1991).
[14] J. W. Swift, S. H. Strogatz, and K. Wiesenfeld, Physica D **55**, 239 (1992).
[15] J. P. Laplante and T. Erneux, J. Phys. Chem. **96**, 4931 (1992).
[16] M. Yoshimoto, K. Yoshikawa, Y. Mori, and I. Hanazaki, Chem. Phys. Lett. **189**, 18 (1992).
[17] J. J. Tyson and S. Kauffman, J. Math. Bio. **1**, 289 (1975).
[18] Y. Kuramoto, Prog. Theor. Phys. Suppl. **79**, 223 (1984).
[19] Y. Kuramoto, *Chemical Oscillations, Waves, and Turbulence* (Springer-Verlag, New York, 1984).
[20] K. Bar-Eli, Physica D **14**, 242 (1985).
[21] S. Shinomoto and Y. Kuramoto, Prog. Theor. Phys. **75**, 1105 (1986).
[22] S. Shinomoto and Y. Kuramoto, Prog. Theor. Phys. **75**, 1319 (1986).
[23] H. Sakaguchi and Y. Kuramoto, Prog. Theor. Phys. **76**, 576 (1986).
[24] H. Daido, Prog. Theor. Phys. **77**, 622 (1987).
[25] H. Daido, Rev. Phys. Lett. **61**, 231 (1988).
[26] S. Omata, Y. Yamaguchi, and H. Shimizu, Physica D **31**, 397 (1988).
[27] Y. Yamaguchi, K. Kometani, and H. Shimizu, J. Stat. Phys. **26**, 719 (1981).
[28] C. Baesens, J. Guckenheimer, S. Kim, and R. S. MacKay, Physica D **49**, 387 (1991).
[29] F. Ali and M. Menzinger, J. Phys. Chem. **96**, 1511 (1992).
[30] S. F. Edwards and P. W. Anderson, J. Phys. F **5**, 965 (1975).